Science Advances

AAAS

advances.sciencemag.org/cgi/content/full/3/9/e1701497/DC1

Supplementary Materials for

Mechanistic basis for the recognition of laminin-511 by α6β1 integrin

Mamoru Takizawa, Takao Arimori, Yukimasa Taniguchi, Yu Kitago, Erika Yamashita, Junichi Takagi, Kiyotoshi Sekiguchi

Published 1 September 2017, *Sci. Adv.* **3**, e1701497 (2017)
DOI: 10.1126/sciadv.1701497

This PDF file includes:

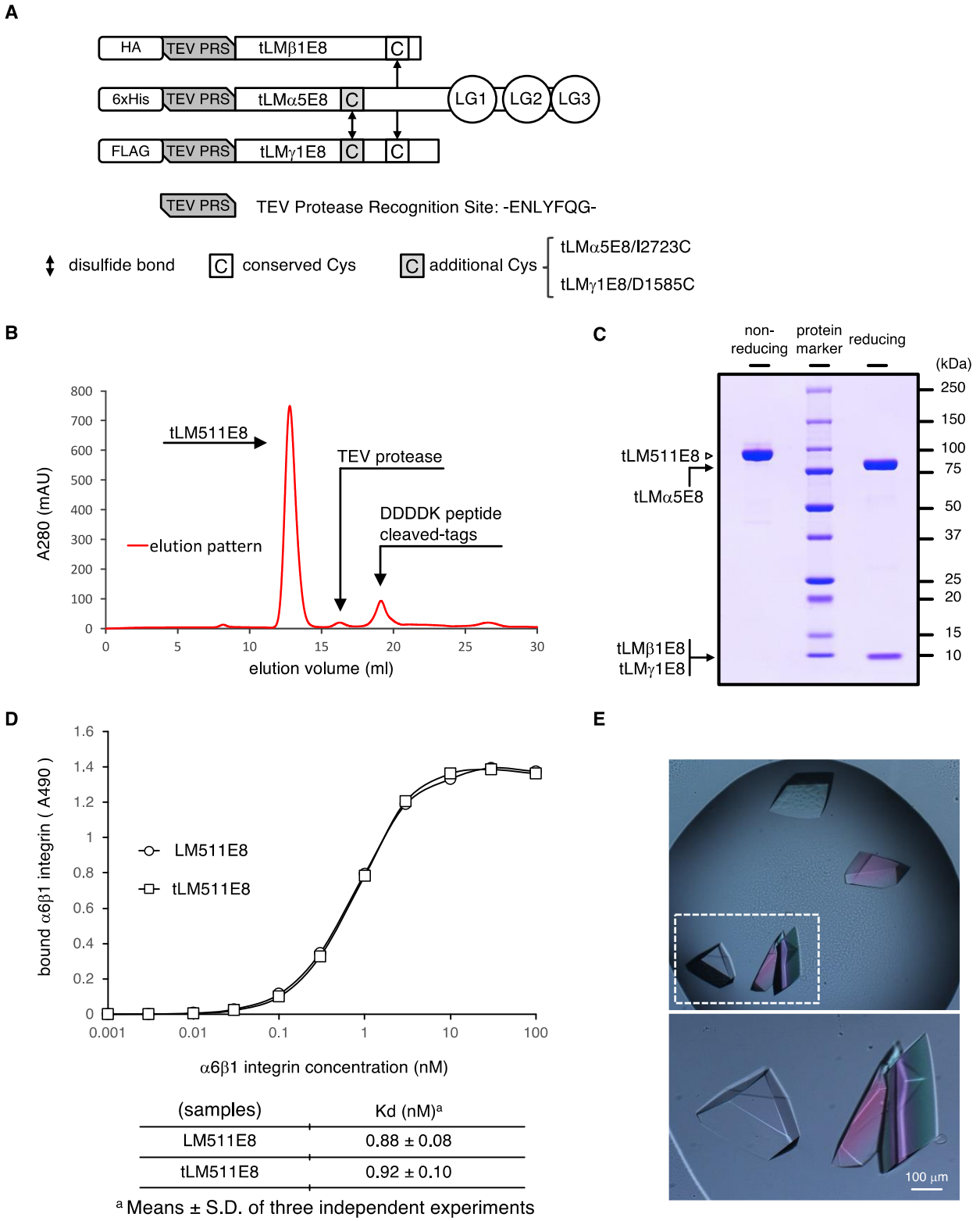

(samples)	Kd (nM)[a]
LM511E8	0.88 ± 0.08
tLM511E8	0.92 ± 0.10

[a] Means ± S.D. of three independent experiments

fig. S1. Preparation and crystallization of tLM511E8. (**A**) Schematic drawing of tLM511E8. To prevent unexpected dissociation of the heterotrimeric coiled-coil assembly in various solvent conditions, an additional disulfide bond was introduced into the coiled-coil by Cys-substitutions for residues α5-

I2723 and γ1-D1585. (**B**) Gel filtration chromatography of TEV protease-treated tLM511E8. (**C**) The peak fraction containing the cleaved tLM511E8 was subject to SDS-PAGE in nonreducing and reducing conditions. (**D**) Microtiter plates were coated with LM511E8 and tLM511E8, and then incubated with α6β1 integrin in the presence of 1 mM $MnCl_2$. The bound integrins were quantified with biotinylated anti-Velcro pAb and HRP-conjugated streptavidin as described in "Materials and Methods". The amounts of integrin bound in the presence of 10 mM EDTA were used as negative controls and subtracted as background. The results are means ± S.D. of three independent experiments. (**E**) Crystals of tLM511E8.

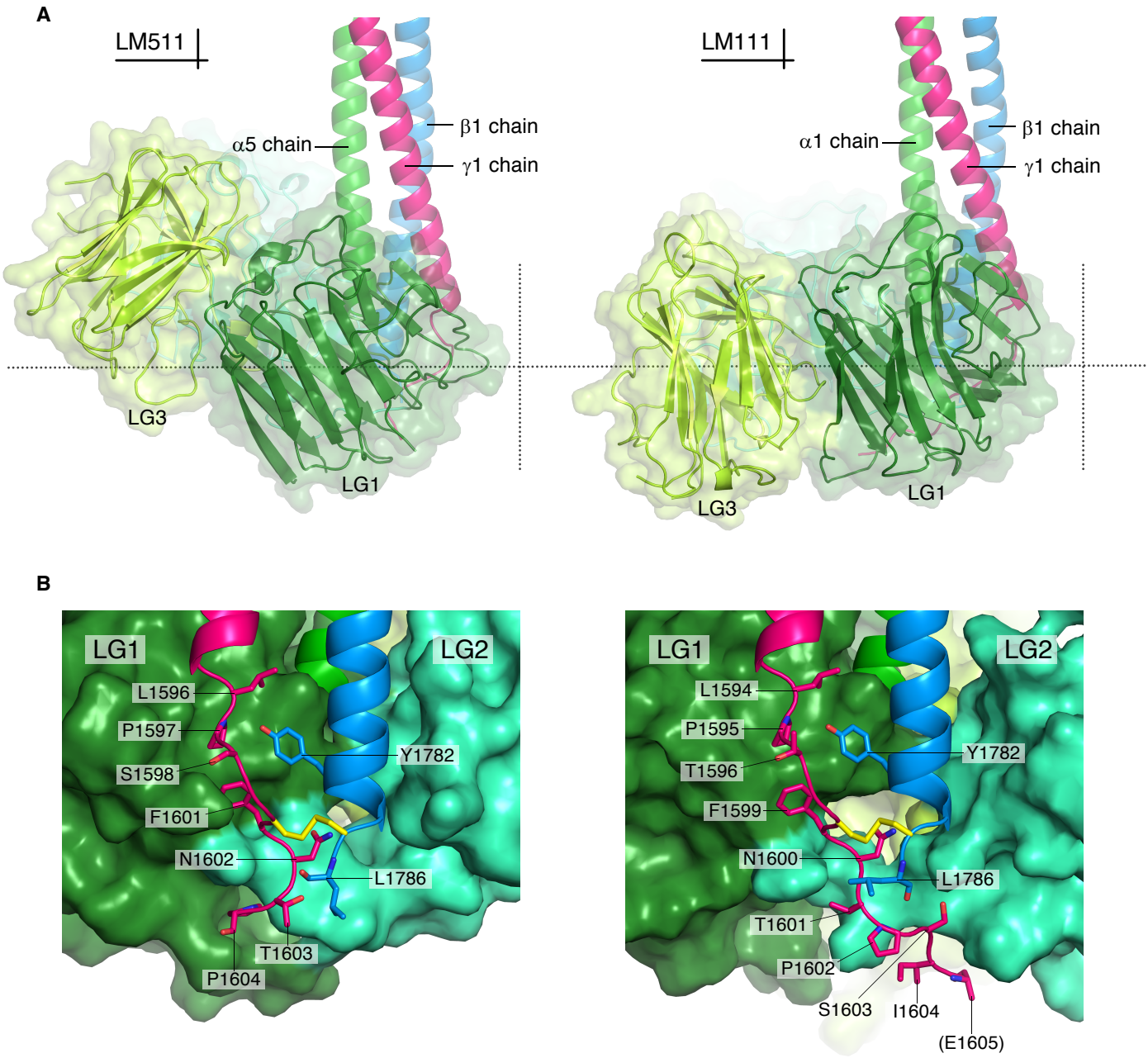

fig. S2. Comparison of the crystal structures of tLM511E8 and mini-E8 of LM111. (**A**) The LG1–LG3 interface of tLM511E8 (*left*) and mini-E8 of LM111 (*right*). (**B**) The β1-γ1 dimer clamped between LG1 and LG2 in tLM511E8 (*left*) and mini-E8 of LM111 (*right*).

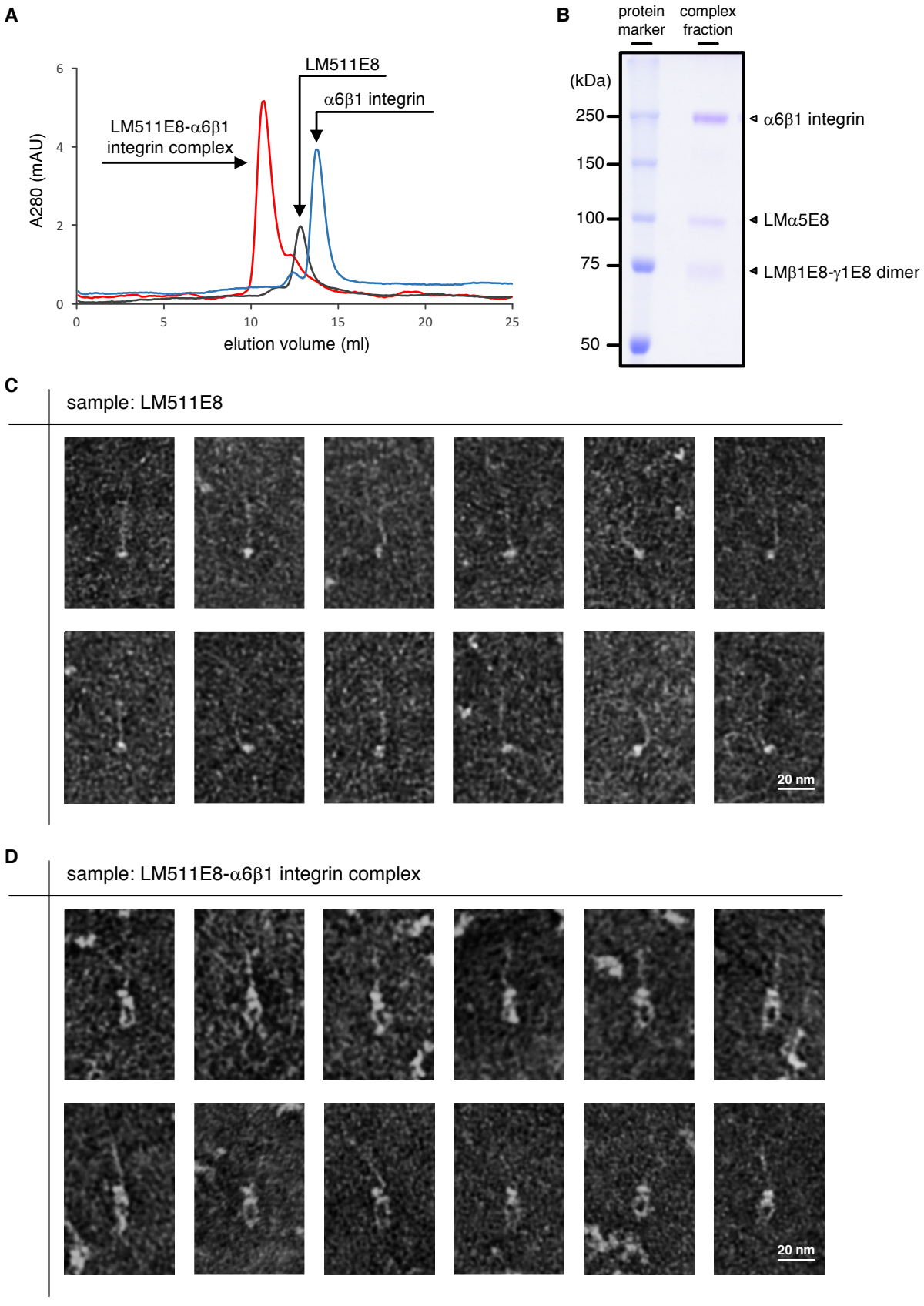

fig. S3. Electron microscopic imaging of the LM511E8–α6β1 integrin complex. (**A**) Elution profiles from gel filtration chromatography for LM511E8 (grey), α6β1 integrin (blue), and LM511E8-α6β1 integrin complex (red). **(B)** The complex fraction was subject to nonreducing SDS-PAGE and CBB staining. (**C**, **D**) Galleries of electron microscopic images of LM511E8 (C) and LM511E8-α6β1 integrin complex (D).

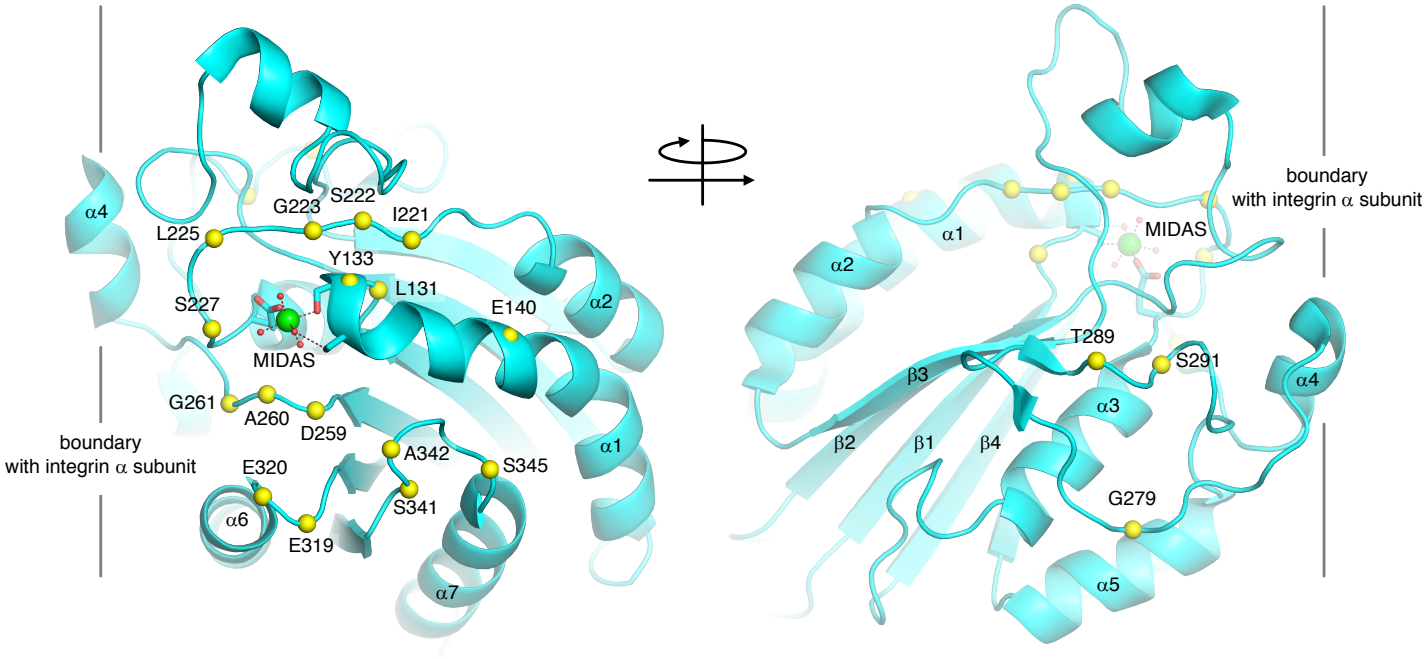

fig. S4. Cys-substituted residues on βI domain. Cα atoms of 19 Cys-substituted residues are marked with yellow spheres on the crystal structure of the βI domain of human integrin β1 (PDB: 4WJK). The metal ion in the metal ion-dependent adhesion site of the integrin β1 (β1-MIDAS) is shown as a green sphere.

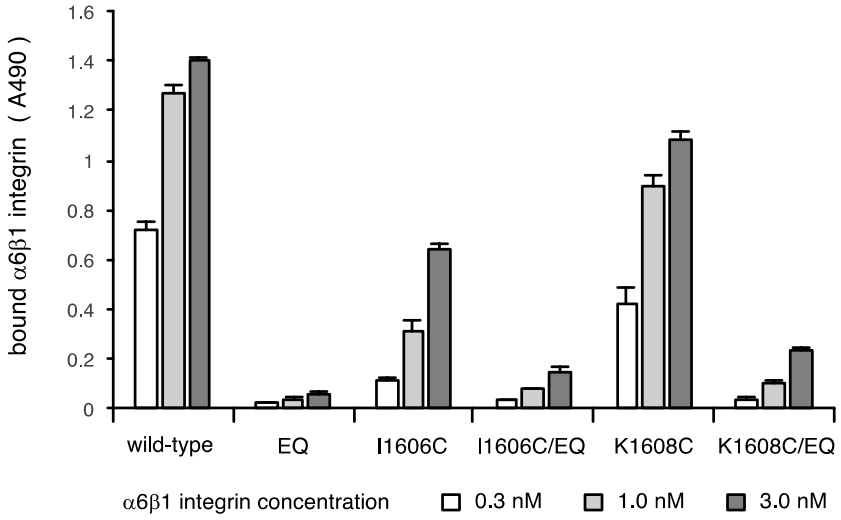

fig. S5. Integrin binding activity of wild-type and Cys-substituted LM511E8s. Microtiter plates were coated with LM511E8/wild-type, LM511E8/I1606C, LM511E8/K1608C, and their E to Q mutants and then incubated with α6β1 integrin in the presence of 1 mM $MnCl_2$. Bound integrins were quantified using biotinylated anti-Velcro pAb and HRP-conjugated streptavidin as described in "Materials and Methods". The amounts of integrin bound in the presence of 10 mM EDTA were used as negative controls and subtracted as background. Each column represents the mean ± S.D. of three independent experiments.

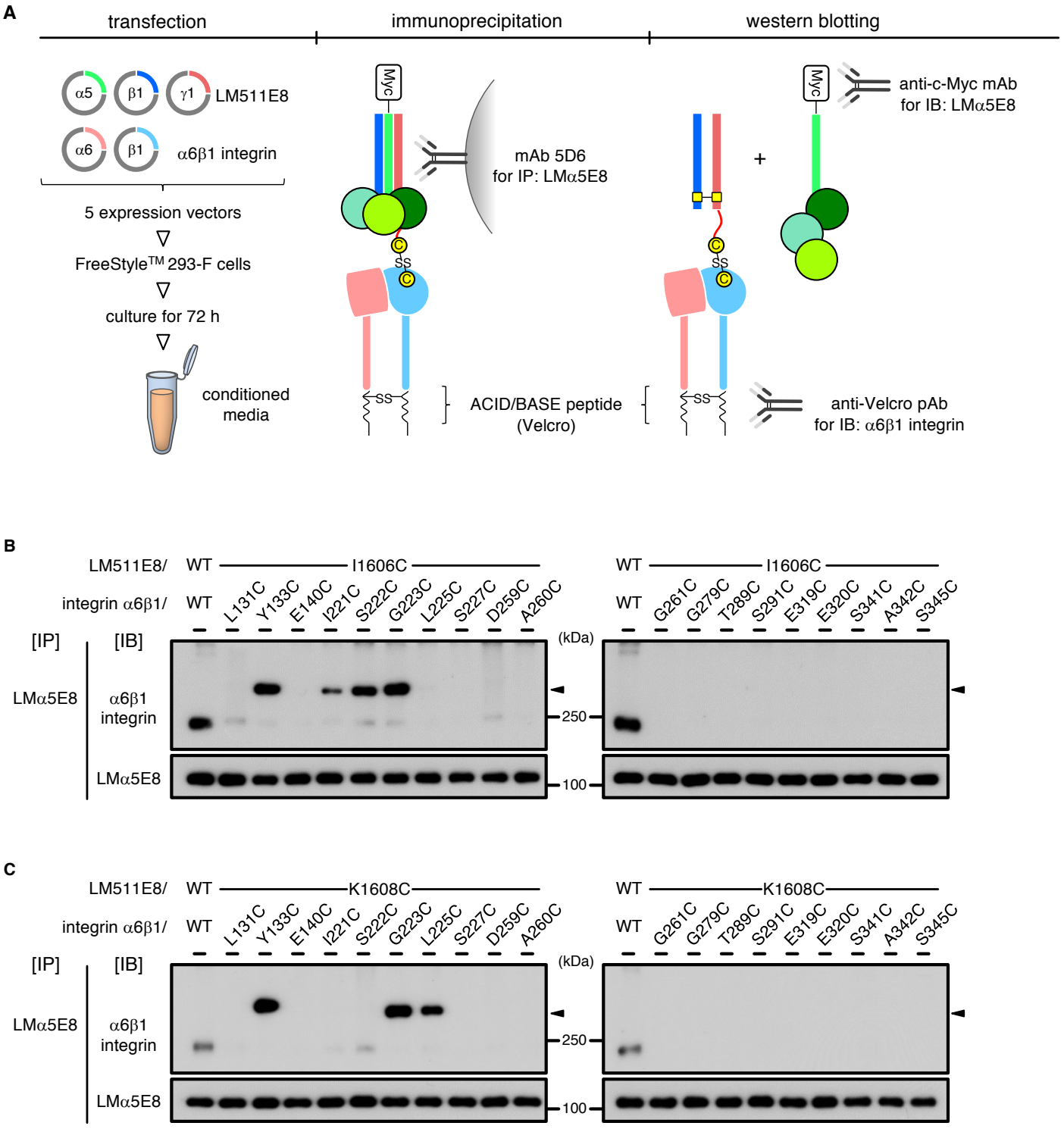

fig. S6. Disulfide formation between Cys-substituted LM511E8 and α6β1 integrin. (**A**) Schematic diagram of the disulfide crosslink assay. LM511E8 and α6β1 integrin were coexpressed in FreeStyle™ 293-F cells (*left*) followed by immunoprecipitation of the secreted LM511E8-α6β1 integrin complex with mAb 5D6 against human laminin α5 chain (*middle*). Immunoprecipitates were subjected to SDS-PAGE in nonreducing conditions and subsequent immunoblotting with anti-Velcro pAb or anti-c-Myc mAb (*right*). (**B**) The results of intermolecular disulfide crosslink assays between LM511E8/I1606C and Cys-substituted α6β1 integrins. (**C**) The results of intermolecular disulfide crosslink assays between LM511E8/K1608C and Cys-substituted α6β1 integrins. Arrow heads indicate disulfide linked products.

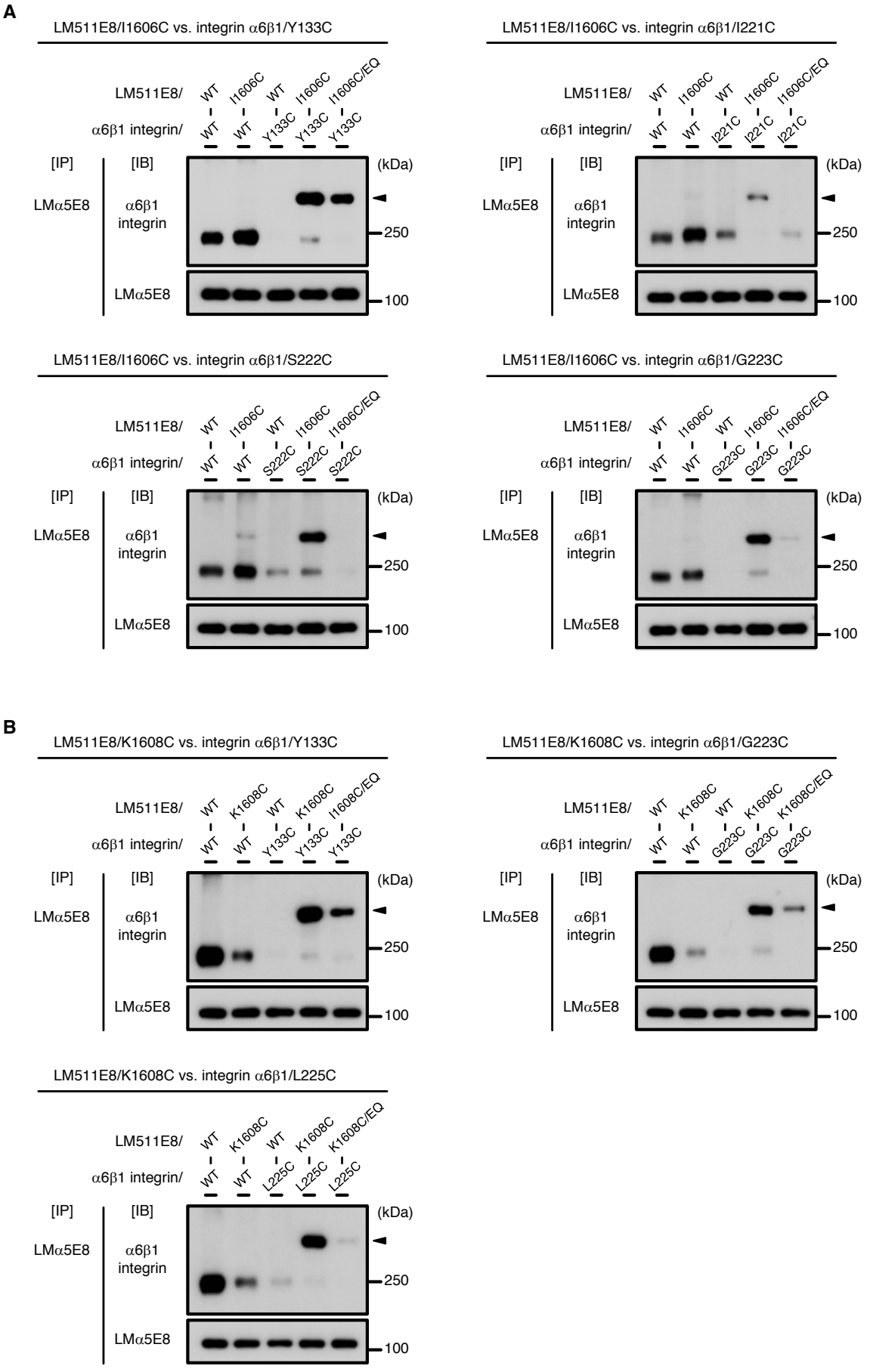

fig. S7. Disulfide cross-link assays using LM511E8/I1606C/EQ and LM511E8/K1608C/EQ. (**A**) Effects of Glu→Gln (EQ) mutation on disulfide formation between LM511E8/I1606C and Cys-substituted α6β1 integrins (Y133C, I221C, S222C, and G223C). (**B**) Effects of the EQ mutation on disulfide formation between LM511E8/K1608C and Cys-substituted α6β1 integrins (Y133C, G223C, and L225C).

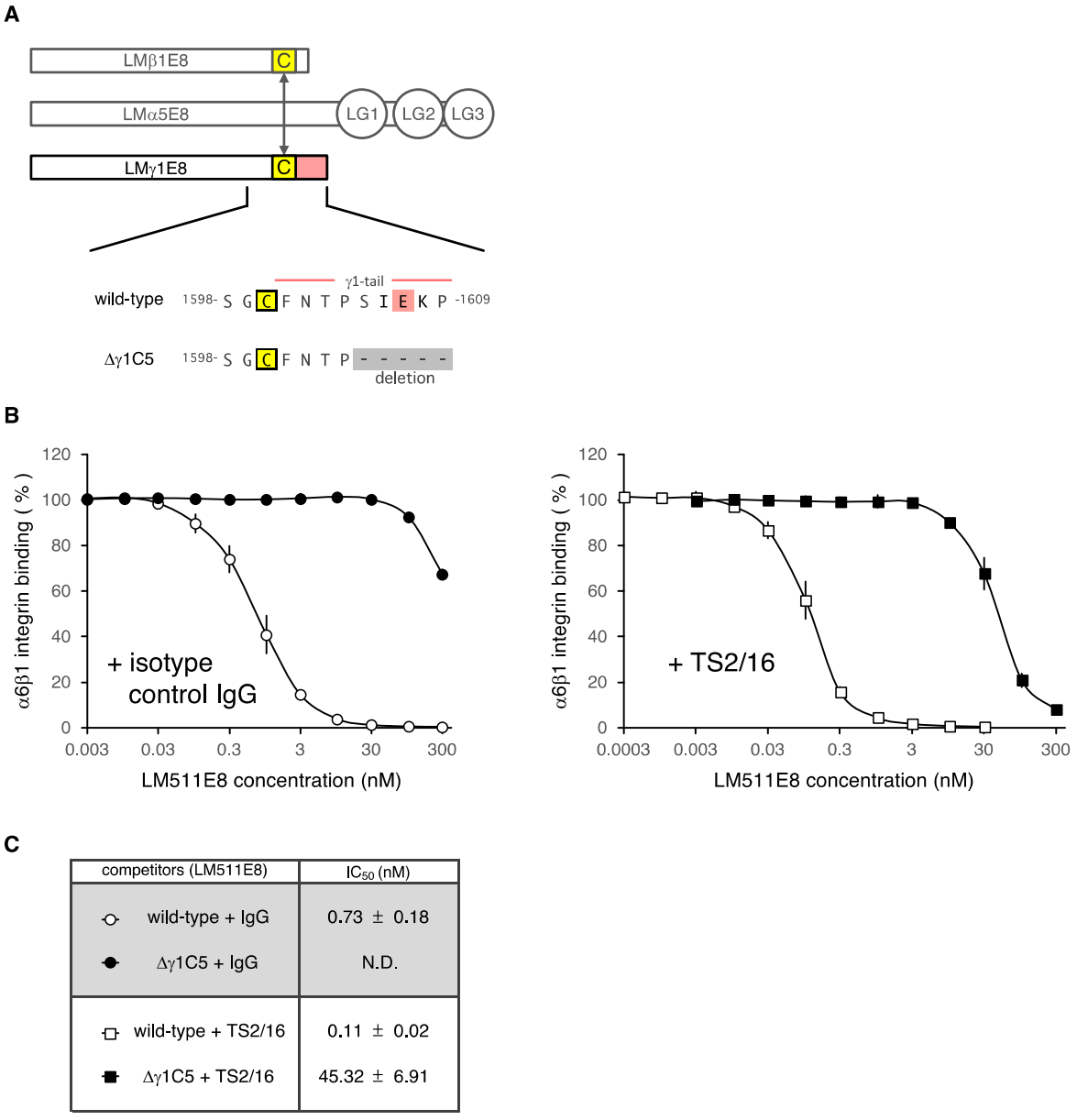

fig. S8. Inhibition of the LM511E8–α6β1 integrin interaction by wild-type and Δγ1C5 LM511E8. (**A**) Schematic drawing of wild-type and Δγ1C5 LM511E8. (**B**) Inhibition of α6β1 integrin binding to LM511E8 by wild-type (white) or Δγ1C5 (black) LM511E8, in the absence (circle) or presence (square) of integrin β1 activating mAb TS2/16. (**C**) IC_{50} values of LM511E8 (means ± S.D. of three independent experiments). N.D., not determined.

table S1. Data collection and refinement statistics.

Data name PDB ID	LM511E8 (for S-SAD)[a]	LM511E8 5XAU
Data collection		
Source	PF BL-1A	SPring-8 BL44XU
Space group	*C*2	*C*2
Cell dimensions		
a, *b*, *c* (Å)	175.4, 122.0, 107.7	175.0, 121.6, 107.6
β (°)	127.6	127.6
Wavelength (Å)	2.7	0.9
Resolution (Å)	50.0 - 2.48 (2.54 - 2.48)	50.0 - 1.80 (1.83 - 1.80)
R_{merge} or R_{sym} (%)[b]	10.3 (133)	6.5 (114)
$\langle I/\sigma(I)\rangle$	20.9 (0.87)	16.7 (1.4)
Completeness (%)	98.3 (87.1)	99.9 (100.0)
Redundancy	16.4 (3.7)	3.8 (3.8)
Refinement		
Resolution (Å)		49.41 - 1.80
No. of reflections		155,954
R_{work} / R_{free} (%)[c]		20.2/23.7
No. of atoms		
Protein		11,383
Ca^{2+}		2
Water		591
Average *B* factors (Å^2)		
Protein		36.2
Ca^{2+}		33.7
Water		36.6
r.m.s. deviations		
Bond length (Å)		0.011
Bond angle (°)		1.47

Values in parentheses correspond to the highest resolution shell.
[a]Three datasets collected from the same crystal were merged.
[b]$R_{sym} = 100\times\Sigma|I_{hkl}-\langle I_{hkl}\rangle|\Sigma I_{hkl}$, $\langle I_{hkl}\rangle$ is the mean value of I_{hkl}.
[c]$R_{work} = 100\times\Sigma||F_o|-|F_c||/\Sigma|F_o|$. R_{free} was calculated from the test set (5% of the total data).